

V. Giurgiutiu
Associate Professor.
Mem. ASME

C. A. Rogers
Dean of Engineering.
Mem. ASME

University of South Carolina,
300 S. Main St.,
Columbia, SC 29208

Z. Chaudhry
United Technologies Research Center,
411 Silver Lane, MS 129-73,
East Hartford, CT 06108

Design of Displacement-Amplified Induced-Strain Actuators for Maximum Energy Output

General stiffness concepts for effective use of induced strain principles as they apply to quasi-static actuation of structures and devices are presented. The conventional induced-strain actuator is first reviewed. The effect of structural elasticity is then discussed. Basic principles of displacement amplification are presented. The influences of structural and amplification elasticity are then discussed. An example of effective induced-strain actuator design with displacement amplification is provided.

1 Introduction

Solid-state induced-strain actuators are extensively studied for a variety of aerospace and mechanical engineering applications (Dadone, 1995; Straub and Merkley, 1995; Steltzner et al. 1995; Bamford et al., 1995). In previous work, Giurgiutiu, Chaudhry, and Rogers (1994a, 1995a) have shown that active vibration control for aeroelastic and other applications is conceptually possible using induced-strain actuators (ISA) instead of conventional hydraulic and/or electro-mechanical devices. Induced-strain actuators have obvious benefits in terms of reliability, autonomy, and compactness. Their energy requirements appear to be within the capabilities of commercially-available ISA devices (Giurgiutiu, Chaudhry, and Rogers, 1996a). However, the problem of amplifying the very small displacement of the induced-strain material (order of 0.1 mm) presents a significant challenge. Displacement amplification concepts are abundant, but conventional displacement amplifiers are usually built without concern for efficient energy transfer. In this paper, we present a step-by-step approach to understanding the sensitive areas of induced-strain actuator design, and achieving effective energy transfer through a displacement amplifier suitable for use in conjunction with commercially-available ISA devices. The development is performed under quasi-static conditions. Extension to dynamic conditions can be readily achieved through the dynamic stiffness concept (Giurgiutiu, Chaudhry, and Rogers, 1994b). Although this research was initially spurred by the needs of aeroelastic vibration control, the results presented in this paper have a much larger arena of applicability. These results can be used in conjunction with the effective design of most induced-strain actuators, either for new applications, or for replacing conventional hydraulic or/and electro-mechanical devices.

2 Conventional Induced-Strain Actuators

Conventional induced-strain actuators are readily available on the commercial market (Giurgiutiu, Chaudhry, and Rogers, 1996a). When activated by electric or magnetic fields, these devices produce an output displacement that is more or less proportional to the applied field. Piezo-electric (e.g., PZT) and electro-strictive ceramics (e.g., PMN) are commonly used in induced-strain actuators employing electric fields. Magneto-strictive materials (e.g., TERFENOL) are used in induced-strain

actuators using magnetic fields. Mechanical modeling of both types of induced-strain actuators is similar, and the generic terminology, induced-strain actuation (ISA) devices, will be used henceforth. Figure 1a shows schematically a conventional induced-strain actuator of internal stiffness k_i , producing an induced-strain displacement u_{ISA} . The internal stiffness, k_i , and the induced-strain displacement, u_{ISA} , also known as free-stroke, are basic characteristics of any ISA device.

2.1 Displacement Analysis. Figure 1a presents an ISA device of internal stiffness k_i acting against an external spring of stiffness k_e . If u_e is the compression of the external spring, k_e , then the force is $F = k_e \cdot u_e$. The force, F , also produces internal compression of the ISA device, i.e., $u_i = F/k_i$. The sum of the internal and external displacements equates the ISA displacement, i.e., $u_i + u_e = u_{ISA}$. This shows that the induced-strain displacement, u_{ISA} , is partly consumed in the internal compressibility of the ISA device, u_i , and partly delivered as useful output displacement, u_e . Upon elimination,

$$u_e = u_{ISA} / (1 + k_e/k_i). \quad (1)$$

Introducing the stiffness ratio, $r = k_e/k_i$, and the output displacement coefficient, $\eta(r) = u_e/u_{ISA}$, one writes $u_e = \eta(r) \cdot u_{ISA}$. Upon substitution, Eq. (1) yields

$$\eta(r) = 1 / (1 + r). \quad (1a)$$

Variation of the output displacement coefficient $\eta(r)$ with stiffness ratio, r , is shown in Fig. 2a. As the external stiffness increases, the fraction of the induced-strain displacement, u_{ISA} , that reaches the output diminishes. For very large external stiffness, one gets the blocked condition, i.e., $u_e \rightarrow 0$, as $r \rightarrow \infty$.

2.2 Energy Analysis. The output energy is the energy delivered by the ISA device into the external spring, i.e.,

$$E_e = \frac{1}{2} k_e \cdot u_e^2. \quad (2)$$

Upon substitution,

$$E_e = [r(1+r)^{-2}] (\frac{1}{2} k_i u_{ISA}^2). \quad (3)$$

Note that the output energy expression given in Eq. (3) consists of a variable coefficient that depends on the stiffness ratio, r , and a constant energy term that depends only on the free stroke, u_{ISA} , and internal stiffness, k_i , of the induced-strain device. Since u_{ISA} and k_i are reference parameters of the induced-strain

Contributed by the Reliability, Stress Analysis & Failure Prevention Committee for publication in the JOURNAL OF MECHANICAL DESIGN. Manuscript received Jan. 1996; revised July 1997. Associate Technical Editor: E. Sancaktar.

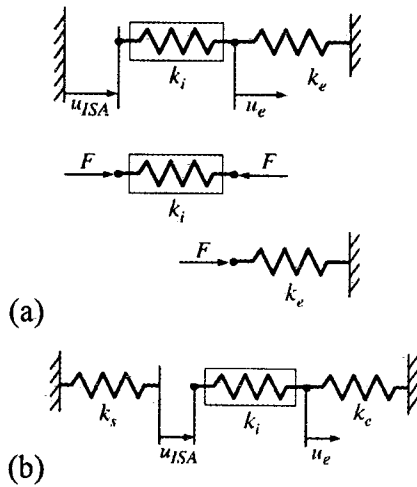


Fig. 1 Schematic representation of a conventional induced-strain actuator: (a) with rigid support (b) with compliant support

device, we call the latter term of Eq. (3) the reference energy of the induced-strain device, i.e.,

$$E_{ref} = \frac{1}{2}k_i \cdot u_{ISA}^2 \quad (4)$$

Values for the reference energy, E_{ref} , and for its specific values per unit volume and unit mass for commercially-available ISA devices were given by Giurgiutiu, Chaudhry, and Rogers (1995b). Maximum output energy values around 2.7 J were found. Maximum energy densities per unit volume and unit mass around 21 J/dm³ and 2.7 J/kg, respectively, were also recorded.

The variable term in Eq. (3) is the output energy coefficient, $E'_e = E_e/E_{ref}$, i.e.,

$$E'_e(r) = r(1+r)^{-2} \quad (5)$$

The governing design factor in the construction of a conventional ISA device is the stiffness ratio, r . Variation of the displacement and energy coefficients with the stiffness ratio, r , is given in Fig. 2(a). The maximum displacement output is obtained as r approaches zero, i.e., when the external stiffness is so weak that practically no resistance is presented to the ISA device and hence the full induced-strain displacement, u_{ISA} , is delivered externally. This case is of limited interest for actuator applications since the actuation force is zero and no output energy is delivered. In the other extreme, when the external stiffness is very much greater than the internal stiffness, the output force is maximum, but the output displacement is zero. Hence, the output energy is again zero. Between these two extremes, an optimum solution may be reached. By differentiating the energy coefficient with respect to the stiffness ratio, r ,

$$\frac{dE'_e}{dr} = 0 \rightarrow 1 - \frac{2r}{1+r} = 0 \rightarrow r_{opt} = 1 \quad (6)$$

This is the well-known stiffness match principle. When the external stiffness matches the internal stiffness, the energy output is maximum and its value is $E_e = \frac{1}{4}E_{ref}$.

3 Induced-Strain Actuators With Support Elasticity

Figure 1b shows schematically an induced-strain actuator in which the support structure is not infinitely rigid. A stiffness value, k_s , is assumed to be present at the support end of the

ISA device. The presence of finite support stiffness, k_s , can significantly modify the output displacement and output energy of the induced-strain actuator, as seen in the following analysis.

3.1 Displacement Analysis. The induced-strain displacement, u_{ISA} , is consumed in the support stiffness, k_s , in the internal stiffness of the actuator, k_i , and in the external stiffness, k_e , i.e., $u_{ISA} = F/k_s + F/k_i + u_e$, $F = k_e \cdot u_e$. Upon elimination,

$$u_e = (1 + k_e/k_s + k_e/k_i)^{-1} \cdot u_{ISA} \quad (7)$$

Introducing the structural stiffness coefficient, $r_s = k_s/k_i$, we write the output displacement coefficient, η , as a function of both r and r_s , i.e.,

$$\eta(r, r_s) = 1/[1 + r(1 + 1/r_s)] \quad (8)$$

The output displacement, u_e , is expressed in terms of the reference (free-stroke) displacement, u_{ISA} , as:

$$u_e = \eta(r, r_s) \cdot u_{ISA} \quad (9)$$

It can be seen that the output displacement coefficient, η , increases as r_s increases, i.e., a stiffer support will give a better displacement output. As $r_s \rightarrow \infty$, the expression of η approaches the simpler expression $\eta(r) = 1/(1 + r)$, which was derived in the previous section as Equation (1a).

3.2 Energy Analysis. The output energy delivered by the induced-strain device is, as before, $E_e = (1/2)k_e \cdot u_e^2$. Upon substitution,

$$E_e = r/[1 + r(1 + 1/r_s)]^{-2} \cdot (\frac{1}{2}k_i \cdot u_{ISA}^2) \quad (10)$$

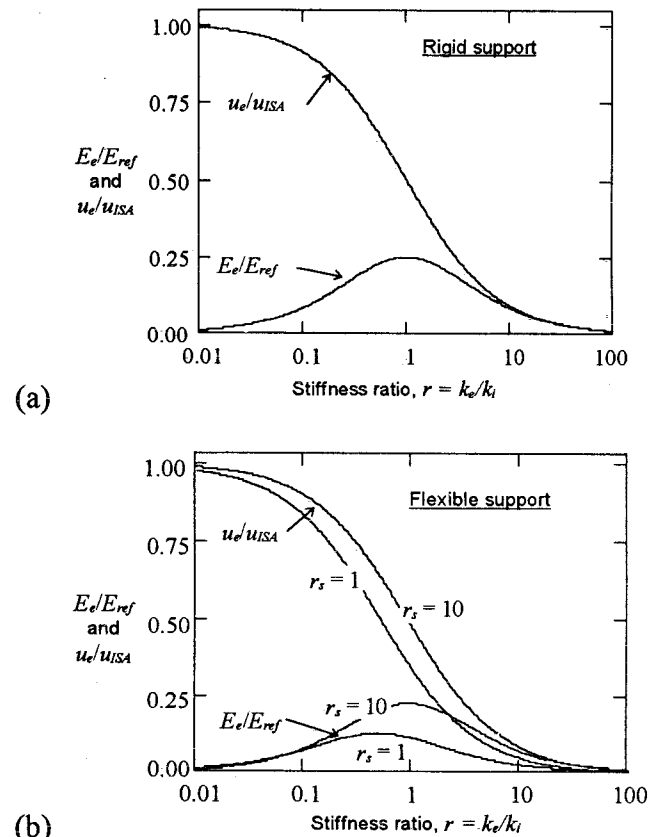


Fig. 2 Variation of output displacement coefficient, $\eta = u_e/u_{ISA}$, and output energy coefficient, $E'_e = E_e/E_{ref}$, with stiffness ratio, $r = k_e/k_i$: (a) rigid support (b) flexible support with various values of the support stiffness ratio, r_s

The last parenthesis in Eq. (10) is the reference energy, E_{ref} , defined by Eq. (4). Dividing Eq. (10) by E_{ref} yields the expression of the output energy coefficient,

$$E'_e(r, r_s) = r/[1 + r(1 + 1/r_s)]^{-2}. \quad (11)$$

Note that the output energy coefficient depends on both the stiffness ratio, r , and the structural stiffness coefficient, r_s . Figure 2b presents the variations of the displacement and energy coefficients with the stiffness ratio, r , for two values of the structural stiffness coefficient, $r_s = 10$, and $r_s = 1$. For the case of "stiff" support ($r_s = 10$), the displacement and energy curves in Fig. 2(b) are almost identical with those discussed in the previous section for an induced-strain actuator with rigid support. For the case of "elastic" support ($r_s = 1$), a significant shift is observed in the output displacement and output energy curves. More importantly, the peak of the output energy curve is reduced by about a factor of 2. This 50 percent reduction in energy output is explainable, since half of the available energy ends up as elastic energy stored in the support.

4 Displacement-Amplified Induced-Strain Actuators

4.1 Displacement Analysis. Displacement amplifiers are currently used to boost the output of ISA devices. The simplest displacement amplification concept is that of a lever with unequal arms (Fig. 3(a)). This simple concept can be used to analyze even more complicated displacement amplifiers (flex-tensional, deformable triangles, hydrostatic, etc.). At the input end, the lever is actuated by an ISA device (internal stiffness k_i) producing the induced-strain displacement u_{ISA} . The displacement of the input lever arm is $u_{ISA} = F_i/k_i$, where F_i is the force in the ISA device. This displacement produces rotation θ of the lever and hence,

$$l_i \theta = u_{ISA} = F_i/k_i. \quad (12)$$

If the amplifying lever is considered rigid, then the displacement at the output arm, u_e , is given by simple rigid body rotation, i.e.,

$$u_e = l_e \theta. \quad (13)$$

where u_e is the external displacement. For an equivalent external stiffness k_e , the external reaction, F_e , is:

$$F_e = k_e u_e. \quad (14)$$

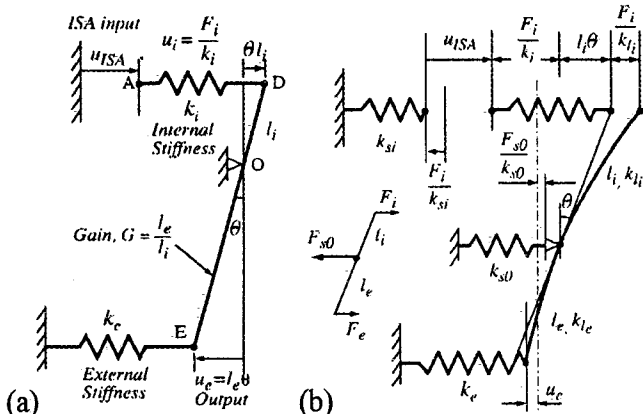


Fig. 3 Conceptual models for displacement-amplified induced-strain actuators: (a) rigid support and amplification mechanism (b) elastic support and amplification mechanism.

The input force, F_i , and the output reaction, F_e , satisfy the lever equilibrium relation:

$$F_i \cdot l_i = F_e \cdot l_e, \quad (15)$$

where l_i and l_e are the lever arms connected to the internal and external displacements, respectively. Introducing the kinematic gain:

$$G = l_e/l_i, \quad (16)$$

one expresses the internal force in terms of the external reaction, and vice-versa, i.e.,

$$F_i = G \cdot F_e, \quad \text{and} \quad F_e = F_i/G. \quad (17)$$

Eliminating θ between Eqs. (12) and (13), and using Eqs. (14) through (17), yields

$$u_e = G(1 + G^2 k_e/k_i)^{-1} u_{ISA}. \quad (18)$$

Using the definitions $r = k_e/k_i$ and $\eta = u_e/u_{ISA}$, one writes the output displacement coefficient:

$$\eta(G, r) = G/(1 + r \cdot G^2). \quad (19)$$

The output displacement coefficient, $\eta(G, r)$, is always less than the kinematic gain, G , since part of the amplification effect is always lost due to the internal compliance of the induced-strain device.

4.2 Output Energy Analysis. The energy output from a displacement-amplified induced-strain actuator is simply the energy stored in the external spring, i.e.,

$$E_e = \frac{1}{2} k_e u_e^2. \quad (20)$$

Substituting $k_e = r \cdot k_i$ and $u_e = \eta \cdot u_{ISA}$ into Eq. (20), and using Eq. (19), yields:

$$E_e = [r \cdot G^2 / (1 + r \cdot G^2)^2] \cdot (\frac{1}{2} k_i \cdot u_{ISA}^2). \quad (21)$$

Dividing the output energy, E_e , by the reference energy, $E_{ref} = (1/2) k_i \cdot u_{ISA}^2$, one gets the expression of the output energy coefficient, E'_e , for a displacement-amplified induced-strain actuator:

$$E'_e = r G^2 / (1 + r G^2)^2. \quad (22)$$

The energy coefficient is a function of both the stiffness ratio, r , and the kinematic gain, G . Figure 4 shows plots of the energy coefficient vs. stiffness ratio, r , for various values of the kinematic gain, G . For $G = 1$, i.e., for an ISA device without amplification, the peak value of the energy coefficient is reached for $r_{opt} = 1$, i.e., the stiffness match concept. For values of G greater than 1, i.e., for devices with displacement amplification, the value of the optimal stiffness ratio, r_{opt} , changes, and the peak energy output is reached at lower values of r_{opt} . For a ten times kinematic gain ($G = 10$), the optimal stiffness ratio is about 1/100. Exact expressions of the optimal stiffness ratio in terms of the kinematic gain, G , are obtained by differentiating the energy coefficient with respect to r , and setting the derivative equal to zero, i.e.,

$$\frac{d}{dr} E'_e = [G^2 / (1 + r \cdot G^2)^2] \cdot \left(1 - 2r \frac{G^2}{1 + r \cdot G^2} \right) = 0,$$

$$\text{hence } r_{opt} = 1/G^2. \quad (23)$$

Conversely, for fixed external η and internal stiffness values, the optimum gain is

$$G_{opt} = 1/\sqrt{r}. \quad (23a)$$

The output displacement coefficient (overall amplification ratio), corresponding to the optimum kinematic gain, is ob-

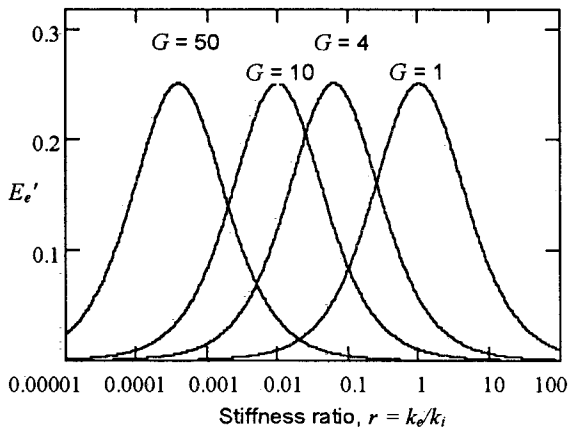


Fig. 4 Output energy coefficient E_e' , versus stiffness ratio, $r = k_e/k_i$, for various values of the kinematic gain, G

tained by substituting the expression of G_{opt} into Eq. (19) for η . Upon simplification,

$$\eta_{opt} = 0.5/\sqrt{r}. \quad (24)$$

It should be noted that the value of the optimum amplification ratio, η_{opt} , is half the value of the optimum gain, G_{opt} . To obtain a certain overall amplification ratio at the optimum operating point, one has to provide twice as much kinematic gain in the internal construction of the displacement amplifier. Plots of the optimal kinematic gain, G_{opt} , and of the amplification ratio, η_{opt} , versus the inverse stiffness ratio, $1/r$, are given in Fig. 5.

4.3 Optimal Kinematic Gain, G , for a Given Value of η . When the output displacement coefficient, $\eta = u_e/u_{ISA}$, and the stiffness ratio, $r = k_e/k_i$, are specified, the value of the kinematic gain, G , must be selected. The expression of the output displacement coefficient given in Eq. (19) can be solved for a given η to obtain the desired value of G . A plot of η vs. G for a fixed value of r is given in Fig. 6. The kinematic gain, G , that will produce a required output displacement coefficient, η , is obtained by intersecting the $\eta - G$ curve of Fig. 6 with an $\eta = \text{const.}$ line. Figure 6 shows that two solutions, G_1 and G_2 , are generally possible. The same result can be obtained symbolically by solving Eq. (31): One gets the two solutions of a quadratic equation in G , containing the \pm sign. Of the two possible solutions for G , only one is optimal (Giurgiutiu, Chaudhry, and Rogers, 1994a), i.e.,

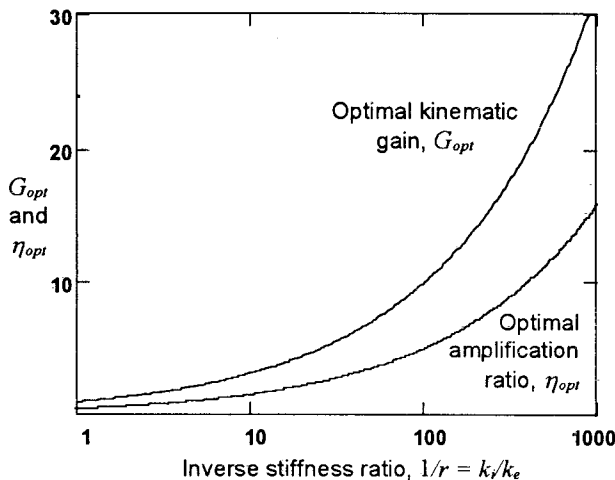


Fig. 5 Optimal kinematic gain and amplification ratio versus inverse stiffness ratio

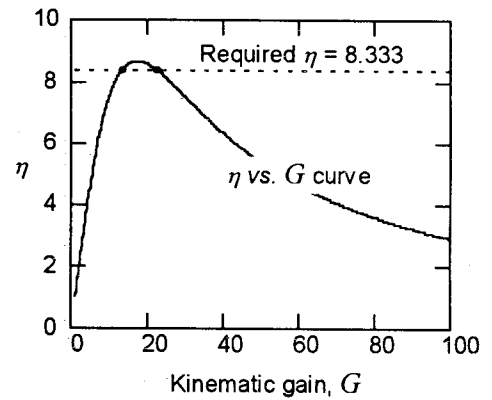


Fig. 6 Variation of output displacement coefficient, η , with kinematic gain, G , for a fixed stiffness ratio, $r = 1/300$

$$G(\eta, r) = \frac{1}{2\eta r} [1 - \sqrt{1 - 4\eta^2 r}]. \quad (25)$$

The sign of the discriminant $1 - 4\eta^2 r$ determines the existence of the solutions. In practical terms this means that, for a given value of the output displacement coefficient, η , and a given stiffness ratio, r , one may or may not be able to construct an actual amplification device depending on the sign of the discriminant. For a given displacement coefficient, real values of the kinematic gain, G , are only obtained if the stiffness ratio, r , satisfies the condition:

$$r \leq r_{cr}, \quad \text{where } r_{cr} = 1/4\eta^2. \quad (26)$$

Real values of the kinematic gain, G , exist only if the internal stiffness of the ISA stack is greater than a critical value, i.e.,

$$k_i \geq (k_i)_{cr}, \quad \text{where } (k_i)_{cr} = k_e/r_{cr}. \quad (27)$$

For $r = r_{cr}$, the kinematic gain, G , takes the value $G_{cr} = 2\eta$. The output energy coefficient, E_e' , given by Eq. (26), can be expressed as:

$$E_e' = \frac{1}{4} \cdot (r/r_{cr}). \quad (28)$$

Figure 7 gives plots of the normalized kinematic gain, $G' = G/G_{cr}$, and output energy coefficient, E_e' , versus the internal stiffness ratio, $k_i/k_e = 1/r$, for a fixed value of the output displacement coefficient, η . The output energy is maximum

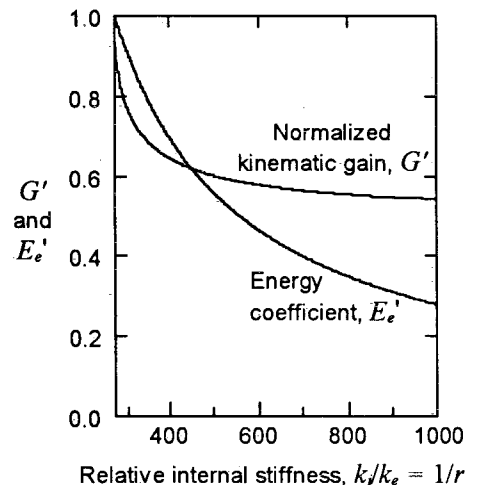


Fig. 7 Variation of normalized kinematic gain, G' , and of output energy coefficient, E_e' , with relative internal stiffness, $k_i/k_e = 1/r$, for a fixed value of η ($\eta = 8.333$)

when the stiffness ratio matches the critical stiffness ratio given by Eq. (26). Hence, the critical stiffness ratio defined by Eq. (26) is actually the optimum stiffness ratio for the displacement-amplified induced-strain actuator. This observation is of utmost importance in the design of a displacement-amplified induced-strain actuator.

Another observation stemming from Fig. 7 is that the behavior of the kinematic gain and of the output energy coefficient around the optimum point is not robust. Small variation in the stiffness ratio can produce large variations in G and E_e . It can be easily verified that the derivative of G with respect to r has an infinite value at the optimum stiffness ratio point, $r/r_{cr} = 1$. The use of optimum stiffness ratio in displacement-amplified induced-strain actuators, though attractive, may not be desirable, since small manufacturing variations easily lead to "detuning" and loss of performance. A design point slightly away from the optimum may offer a better choice from this point of view, and may lead to a more robust behavior.

5 Displacement-Amplified Induced-Strain Actuator With Support and Transmission Elasticity

Real-life displacement-amplified induced-strain actuators incorporate a host of parasitic flexibilities that diminish their performance. The support structure, the lever arms, and the lever fulcrum may present significant compliance. Figure 3b shows these parasitic effects modeled by the finite stiffness values, k_{si} , k_{li} , k_{le} , and k_{s0} . The effect of these parasitic elasticity effects upon the output displacement and output energy of the displacement-amplified induced-strain actuator have also been studied.

5.1 Displacement Analysis. The induced-strain displacement, u_{ISA} , is consumed into the support elasticity, k_{si} , the internal elasticity of the ISA stack, k_i , the elasticity of the input lever arm, k_{li} , the elasticity of the fulcrum support, k_{s0} , and the lever rotation θ . Hence,

$$u_{ISA} = \frac{F_i}{k_{si}} + \frac{F_i}{k_i} + \frac{F_i}{k_{li}} + \frac{F_{s0}}{k_{s0}} + l_i\theta, \quad (29)$$

where F_i is the force in the ISA device, and F_{s0} is the force in the fulcrum support. Note that, at the fulcrum support, one encounters the combined action of the input and output forces, i.e., $F_{s0} = F_i + F_e$. The rotation, θ , produces an amplified displacement, $l_e\theta$, which is distributed into the displacement of the output lever arm, F_e/k_{le} , the displacement of the fulcrum support, F_{s0}/k_{s0} , and the useful output displacement, u_e . Thus,

$$l_e\theta = \frac{F_e}{k_{le}} + \frac{F_{s0}}{k_{s0}} + u_e. \quad (30)$$

Recalling that $F_e = k_e u_e$, and $F_e l_e = F_i l_i$, one eliminates θ between Eqs. (29) and (30), and gets the constitutive relation of the displacement-amplified induced-strain actuator with support and amplification elasticity. Introducing notations for the equivalent input and output stiffness:

$$k_i^* = \left[\frac{1}{k_i} + \frac{1}{k_{li}} + \frac{1}{k_{si}} + \frac{(1+G)}{G} \frac{1}{k_{s0}} \right]^{-1},$$

$$k_e^* = \left[\frac{1}{k_e} + \frac{1}{k_{le}} + (1+G) \frac{1}{k_{s0}} \right]^{-1} \quad (31)$$

yields

$$u_e = G \cdot (k_e/k_e^* + G^2 k_e/k_i^*)^{-1} u_{ISA}. \quad (32)$$

Expression (32) can be simplified by defining the input and output stiffness ratios, r_i^* and r_e^* , as

$$r_i^* = k_e/k_i^*, \quad \text{and} \quad r_e^* = k_e/k_e^*. \quad (33)$$

Hence, the constitutive relation of the displacement-amplified induced-strain actuator with support and amplification elasticity, becomes:

$$u_e = G \cdot (r_e^* + r_i^* \cdot G^2)^{-1} u_{ISA}. \quad (34)$$

The output displacement coefficient, $\eta = u_e/u_{ISA}$, for a displacement-amplified induced-strain actuator with support and amplification elasticity, is

$$\eta = G/(r_e^* + r_i^* \cdot G^2). \quad (35)$$

Note that the displacement amplification coefficient, η , is only a fraction of the kinematic gain, G , since part of the amplification effect is lost in the elasticity of the ISA material, the structural support, and the lever arms. Also note the similarity of Eqs. (35) and (31) giving the displacement amplification coefficient for a displacement-amplified ISA device with and without support and amplification elasticity, respectively. The improved Eq. (35), that takes into account support and amplification elasticity, uses the modified stiffness ratios, r_i^* and r_e^* , defined by Eqs. (30), (31) and (33). When the support and amplification elasticities are ignored, $r_i^* \rightarrow 1$ and $r_e^* \rightarrow r$, and Eq. (35) reduces to the simpler Eq. (31).

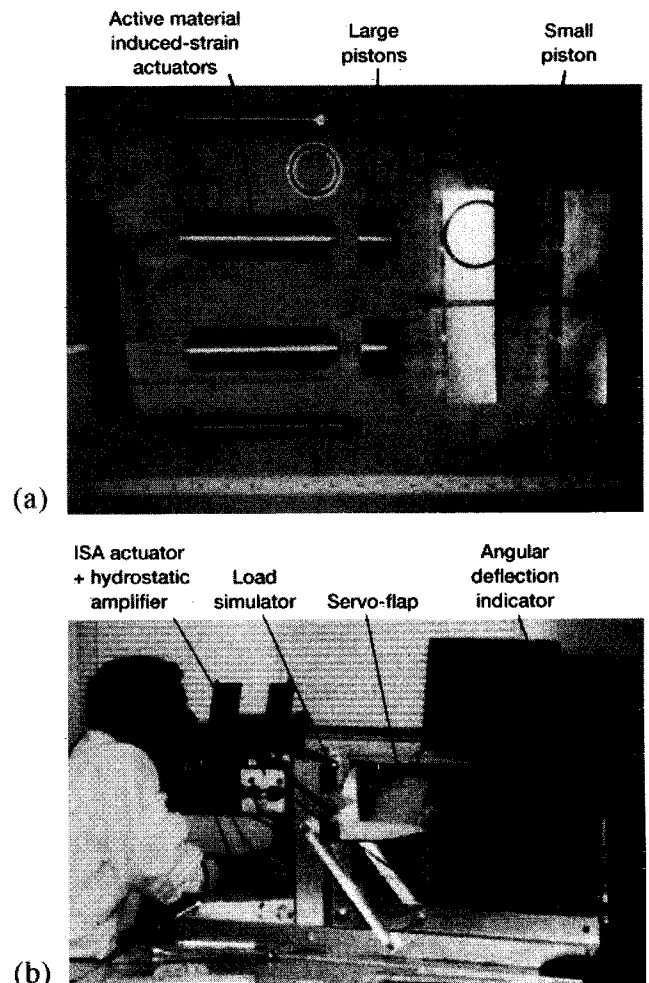


Fig. 8 Hydraulic-amplified high-displacement induced-strain actuator proof-of-concept demonstrator, HAHDIS Mk. 1: (a) internal construction (b) experimental set-up for static and dynamic testing

5.2 Output Energy. Substituting Eq. (35) into Eq. (2), and using $k_e = r \cdot k_i$ and $u_e = \eta \cdot u_{ISA}$, and using the previously derived expression for η , yields the output energy expression for a displacement-amplified induced-strain actuator with support and amplification elasticity:

$$E_e = [r \cdot G^2(r_i^* + r_e^* \cdot G^2)](\frac{1}{2}k_i \cdot u_{ISA}^2). \quad (36)$$

Dividing the output energy, E_e , by the reference energy, $E_{ref} = \frac{1}{2}k_i \cdot u_{ISA}^2$, yields the output energy coefficient, E'_e , in the form:

$$E'_e(r, r_i^*, r_e^*) = r \cdot G^2 / (r_i^* + r_e^* \cdot G^2)^2. \quad (37)$$

In maximizing the output energy coefficient of a displacement-amplified induced-strain actuator with support and amplification elasticity, one needs not only to take into account the conventional conventional stiffness ratio, $r = k_e/k_i$, but also the additional stiffness ratios, $r_i = k_i/k_i^*$ and $r_e = k_e/k_e^*$, that account for the elasticity of the support structure and of the amplification arms.

6 Practical Tests and Experimental Results

To test the present analysis, two proof-of-concept demonstrator models have been designed, built, and tested. Details of this work have already been reported by the authors in other publications (e.g., Giurgiutiu, Chaudhry, and Rogers, 1996b;

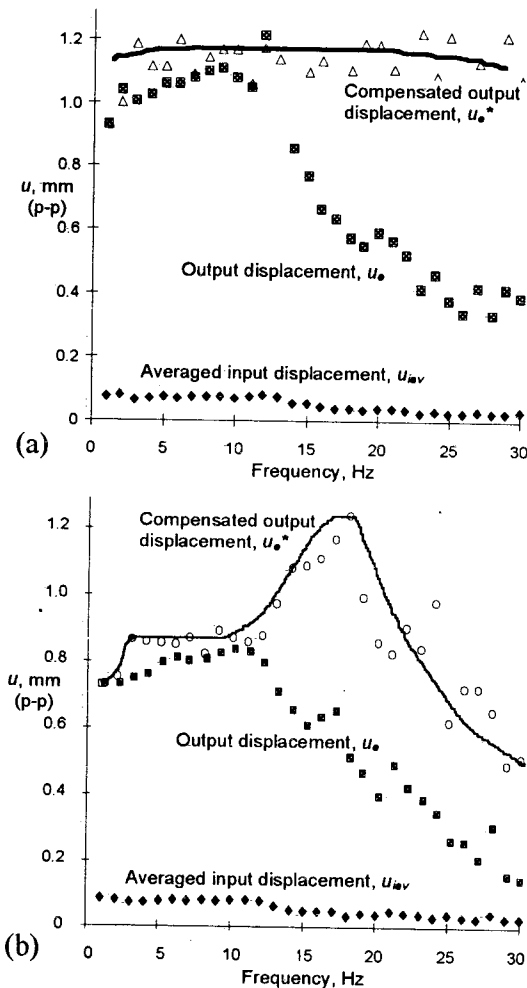


Fig. 9 Frequency response curves of the improved HAHDIS Mk.1a demonstrator in the range 1–30 Hz: (a) no external load (b) low inertial from light realistic flap

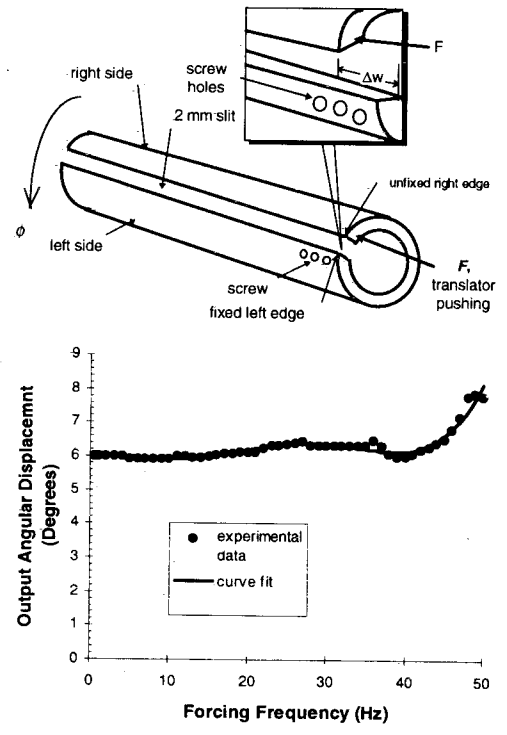


Fig. 10 The LARIS concept for linear-to-rotary conversion and displacement amplification: (a) the twist-warping coupling principle (b) LARIS frequency response curves up to 50 Hz

Giurgiutiu and Rogers, 1997; Giurgiutiu, Rogers, and McNeil, 1997) and hence only a succinct review of the main features will be presented here. These actuators were intended for aerospace solid-state actuation with special interest to the aero-servo-elastic control of vibrations and flutter through solid-state actuated flaps, tabs, and vanes. Two amplification concepts were employed: (a) one concept was based on hydrostatic principles (HAHDIS); (b) the another concept was based on twist-warping coupling in thin-wall open tubes (LARIS).

The HAHDIS Mk 1 proof-of-concept demonstrator (Giurgiutiu, Chaudhry, and Rogers, 1996) consisted of two counteracting active material stacks placed in a boxer configuration and activating large-area input pistons. The volumetric fluid displacements generated by the piezo stacks operated the opposing chambers of an output hydraulic cylinder which performs an oscillatory motion. Since the output cylinder has a much smaller diameter than the input cylinders, hydrostatic amplification is realized with the kinematic gain $G = d_{in}^2/d_{out}^2$. Figure 8 presents the internal construction of the HAHDIS Mk 1 test article (Fig. 8a) and the experimental set up for static and dynamic testing (Fig. 8b). Figure 9 shows the frequency response under no load (Fig. 9a) and inertial load (Fig. 9b). The capability of the HAHDIS device to produce sizable output displacements in excess of 1 mm over a frequency range of up to 30 Hz is apparent.

Remarkable results for angular motion actuation have been shown by the LARIS displacement amplification principle. The warping-torsion coupling of an open-tube structure is utilized to transform and amplify the small axial displacement produced by the induced-strain actuator and to obtain a sizable angular deflection at the device output (Giurgiutiu and Rogers, 1997; Giurgiutiu, Rogers, and McNeil, 1997). Figure 10a shows the principle of the LARIS design, while Fig. 10b demonstrates the excellent frequency response. Almost flat response up to 50 Hz was experimentally recorded, and the output displacement was at least 6° . These two examples are tangible illustration of the power of the induced-strain actuator design methodology presented in the present paper.

7 Conclusions

The induced-strain actuators for aeroelastic vibration control applications need to satisfy stringent weight and energy density requirements. *This paper shows a rational way to meet such requirements in an optimal manner.* The maximization of output energy delivered by an induced-strain actuator can be achieved if careful consideration is given to the interplay of stiffness and displacement taking place inside the actuator. The cases presented and analyzed increased in complexity from a conventional design obeying the well-known stiffness match concept, to more complicated analyses. For displacement-amplified induced-strain actuators, a comprehensive analysis tool was developed and presented. Modulation of the stiffness ratio by the kinematic amplification gain was quantified. Design guidelines and a design example were provided. The influence of support and amplification elasticity were included in the expanded formulation of our analysis and are readily available for design use. It was found that support elasticity can adversely modulate the stiffness match concept and dramatically decrease the output effectiveness. Values of support stiffness at least ten times greater than the internal stiffness of the ISA device are necessary to maintain this loss below 10 percent. A hydraulically-amplified high-displacement induced-strain (HAHDIS Mk. 1) actuator was designed and built as a full-scale proof-of-concept demonstrator. Static and dynamic tests have confirmed the analysis. Good frequency response was measured over the range 0–30 Hz. In another application, the LARIS actuator based on warping-torsion coupling, produced in excess of 6° displacement over the 0–50 Hz frequency range.

8 Acknowledgments

The authors gratefully acknowledge the support of the U.S. Army Research Office—University Research Initiative Program, Grant No. DAAL 03-92-G-0180, Dr. Gary Anderson, Program Manager.

9 References

1 Dadone, L., 1995, "An Overview of Smart Structures Materials Applications to Rotor Blades," *2nd Army Workshop on Smart Structures and Materials, University of Maryland, College Park, MD, September 5–7, 1995.*

2 Straub, F. K., and Merkley, D. J., 1995, "Design of a Smart Material Actuator for Rotor Control," *1995 SPIE North American Conference on Smart Structures and Materials, Smart Structures and Integrated Systems, 26 February–3 March 1995, San Diego, CA, Paper #2443-10, in press.*

3 Steltzner, A. D., O'Brien, J., Wada, B. K., and Darrah, S., 1995, "Toughened PZT Composite-Actuator Program," *Proceedings of the 36th AIAA/ASME/ASCE/AHS/ASC Structures, Structural Dynamics, and Materials Conference and Adaptive Structures Forum, New Orleans, LA, April 13–14, 1995, Paper #AIAA-95-1106, pp. 3269–3277.*

4 Bamford, R., Kuo, C. P., Glaser, R., and Wada, B. K., 1995, "Long Stroke Precision Actuator," *Proceedings of the 36th AIAA/ASME/ASCE/AHS/ASC Structures, Structural Dynamics, and Materials Conference and Adaptive Structures Forum, New Orleans, LA, April 13–14, 1995, Paper #AIAA-95-1107, pp. 3278–3284.*

5 Giurgiutiu, V., Chaudhry, Z., and Rogers, C. A., 1994a, "Active Control of Helicopter Rotor Blades with Induced-Strain Actuators," *35th AIAA/ASME/ASCE/AHS/ASC Structures, Structural Dynamics, and Materials Conference and Adaptive Structures Forum, Hilton Head, SC, pp. 288–298, April 18–22, 1994.*

6 Giurgiutiu, V., Chaudhry, Z., and Rogers, C. A., 1994b, "The Analysis of Power Delivery Capability of Induced-Strain Actuators for Dynamic Applications," *ICIM'94, 2nd International Conference on Intelligent Materials, Technomic Pub. Co., pp. 565–576, 1994.*

7 Giurgiutiu, V., Chaudhry, Z., and Rogers, C. A., 1994c, "Efficient Use of Induced-Strain Actuators in Aeroelastic Active Control," *Proceedings of the Second European Conference on Smart Structures and Materials, SPIE Volume 2361, pp. 273–276, Glasgow, UK, October 12–14, 1994.*

8 Giurgiutiu, V., Chaudhry, Z., and Rogers, C. A., 1995a, "Engineering Feasibility of Induced-Strain Actuators for Rotor Blade Active Vibration Control," *Journal of Intelligent Material Systems and Structures, Vol. 6, No. 5, September 1995, pp. 583–597.*

9 Giurgiutiu, V., Chaudhry, Z., and Rogers, C. A., 1995b, "Issues in the Design and Experimentation of Induced-Strain Actuators for Rotor Blade Aeroelastic Control," *Structural Dynamics and Control—Proceedings of the Tenth VPI&SU Symposium, L. Meirovitch, ed., Virginia Polytechnic Institute and State University Press, 1995, pp. 227–238.*

10 Giurgiutiu, V., Chaudhry, Z., and Rogers, C. A., 1996a, "Energy-based Comparison of Commercially Available Solid State Actuators" *Journal of Intelligent Material Systems and Structures, Vol. 7, No. 1, January 1996, Technomic Pub. Co., pp. 4–14.*

11 Giurgiutiu, V., Rogers, C. A., and Rusovici, R., 1996b, "Solid-State Actuation of Rotor Blade Servo-Flap for Active Vibration Control," *Journal of Intelligent Material Systems and Structures, Vol. 7, No. 2, March 1996, Technomic Pub. Co., pp. 192–202.*

12 Giurgiutiu, V., and Rogers, C. A., 1997, "Large-Amplitude Rotary Induced-Strain (LARIS) Actuator," *Journal of Intelligent Material Systems and Structures, Technomic Pub. Co., Jan. 1997, Vol. 8, No. 1, pp. 41–50.*

13 Giurgiutiu, V., Rogers, C. A., and McNeil, S., 1997, "Static and Dynamic Testing of Large-Amplitude Rotary Induced-Strain (LARIS Mk 2) Actuator," *Journal of Intelligent Material Systems and Structures, Technomic Pub. Co., in press.*